SPARC triggers a cell-autonomous program of synapse elimination

Francisco J. López-Murcia[a,b], Beatrice Terni[a,b], and Artur Llobet[a,b,1]

[a]Laboratory of Neurobiology, Department of Pathology and Experimental Therapeutics, University of Barcelona, L'Hospitalet de Llobregat, Barcelona 08907, Spain; and [b]Bellvitge Biomedical Research Institute (IDIBELL), L'Hospitalet de Llobregat, Barcelona 08907, Spain

Edited by Gerald D. Fischbach, The Simons Foundation, New York, NY, and approved September 1, 2015 (received for review June 25, 2015)

Elimination of the excess synaptic contacts established in the early stages of neuronal development is required to refine the function of neuronal circuits. Here we investigate whether secreted protein acidic and rich in cysteine (SPARC), a molecule produced by glial cells, is involved in synapse removal. SPARC production peaks when innervation of the rat superior cervical ganglion and the tail of *Xenopus tropicalis* tadpoles are remodeled. The formation of new cholinergic synapses in autaptic single-cell microcultures is inhibited by SPARC. The effect resides in the C-terminal domain, which is also responsible for triggering a concentration- and time-dependent disassembly of stable cholinergic synapses. The loss of synaptic contacts is associated with the formation of retracted axon terminals containing multivesicular bodies and secondary lysosomes. The biological relevance of in vitro results was supported by injecting the tail of *Xenopus tropicalis* tadpoles with peptide 4.2, a 20-aa sequence derived from SPARC that mimics full-length protein effects. Swimming was severely impaired at ∼5 h after peptide application, caused by the massive elimination of neuromuscular junctions and pruning of axonal branches. Effects revert by 6 d after injection, as motor innervation reforms. In conclusion, SPARC triggers a cell-autonomous program of synapse elimination in cholinergic neurons that likely occurs when protein production peaks during normal development.

neuron–glia interaction | synapse elimination | SPARC | *Xenopus tropicalis* | cholinergic synapse

Synapse elimination is a fundamental process required for refining the function of neuronal circuits. Although the molecular mechanisms involved are largely unknown, several lines of evidence support a prominent role for glial cells. Glia engulf synaptic debris in the *Drosophila* mushroom body during metamorphosis (1), and astrocytes, migroglia, and terminal Schwann cells phagocytose retracted axon bulbs (2–5); however, whether glial cells mediate only the last step of synapse remodeling, which requires phagocytosis, or also participate in synaptic disassembly and subsequent axon retraction, is unclear. Pathways involved in synapse elimination include the classical complement cascade (6, 7) and increased lysosomal activity (8), but the definition of a specific trigger remains elusive.

Given that glial cell-secreted molecules, such as thrombospondin, hevin, and glypicans, favor the establishment of synaptic contacts in the initial stages of synaptogenesis (9–11), we considered the possibility that a similar molecule participates in the initiation of synapse elimination. Our candidate was secreted protein acidic and rich in cysteine (SPARC), a matricellular protein released by astrocytes, microglia, and Schwann cells. SPARC production peaks during the assembly of neuronal circuits and may be involved in various developmental processes of the nervous system, such as angiogenesis, neurogenesis, and neuronal migration (12). Previous studies have suggested that SPARC plays a specific role in synaptic development by (*i*) preventing recruitment of GluA1 and GluA2 AMPA receptor subunits (13), (*ii*) antagonizing the synaptogenic action of hevin (10), and (*iii*) arresting cholinergic presynaptic terminals to an immature stage (14). This evidence supports the role of SPARC as an inhibitory cue of synapse development.

Based on its high degree of conservation among vertebrates, we investigated the role of SPARC on synapse elimination in two vertebrate structures: the rat superior cervical ganglion and the tail of *Xenopus tropicalis* larvae. In both experimental systems, SPARC production is maximal over the period during which cholinergic innervation is refined. Using single-cell microcultures (SCMs), which allow the investigation of cholinergic synapses in vitro in the absence of glia (15), we show that SPARC triggers an acute, concentration-dependent retraction of mature axon terminals. The effect of SPARC on synapse disassembly is further supported by the ability of a SPARC-derived peptide to promote transient elimination of neuromuscular junctions in the tails of living tadpoles.

Results

Maximum SPARC Production Is Associated with Periods of Cholinergic Synapse Elimination. We investigated postnatal changes in SPARC production in the rat superior cervical ganglion, where the protein was concentrated around synaptic contacts (Fig. 1*A*). The highest SPARC levels were found 0.68 ± 0.1 μm away from putative presynaptic terminals ($n = 23$; Fig. 1*B*). Low protein amounts were detected immediately after birth, when ganglionic innervation is maximal (16). As development proceeded, SPARC levels increased, reaching a peak at 1–3 wk of postnatal life (Fig. 1*C* and Fig. S1). This time window coincides with the period of ganglionic synapse elimination reported in rats (17) and hamsters (18). SPARC production was again low in adults, suggesting that maximal protein levels are relevant for refinement of cholinergic innervation in sympathetic ganglia.

Given the high conservation of SPARC through metazoan evolution (19), we considered the possibility that the observed developmental changes in SPARC secretion could be important

Significance

Neuronal circuits require eliminating the excess of synaptic connectivity to acquire complete functionality. Here we show that secreted protein acidic and rich in cysteine (SPARC), a molecule secreted exclusively by glia, is a trigger for synapse elimination. Acting through a region located in its C-terminal domain, SPARC activates synapse disassembly and formation of retracted axon terminals in cholinergic neurons in vitro. The onset of this cell-autonomous program in the tails of living tadpoles drives a loss of motor innervation, causing transient paralysis. We propose that along with their well-established role in ending the process of synapse elimination by engulfing retracted terminals, glia can also act as a trigger through the release of specific molecules, such as SPARC.

Author contributions: A.L. designed research; F.J.L.-M., B.T., and A.L. performed research; F.J.L.-M., B.T., and A.L. analyzed data; and A.L. wrote the paper.

The authors declare no conflict of interest.

This article is a PNAS Direct Submission.

[1]To whom correspondence should be addressed. Email: allobet@ub.edu.

This article contains supporting information online at www.pnas.org/lookup/suppl/doi:10.1073/pnas.1512202112/-/DCSupplemental.

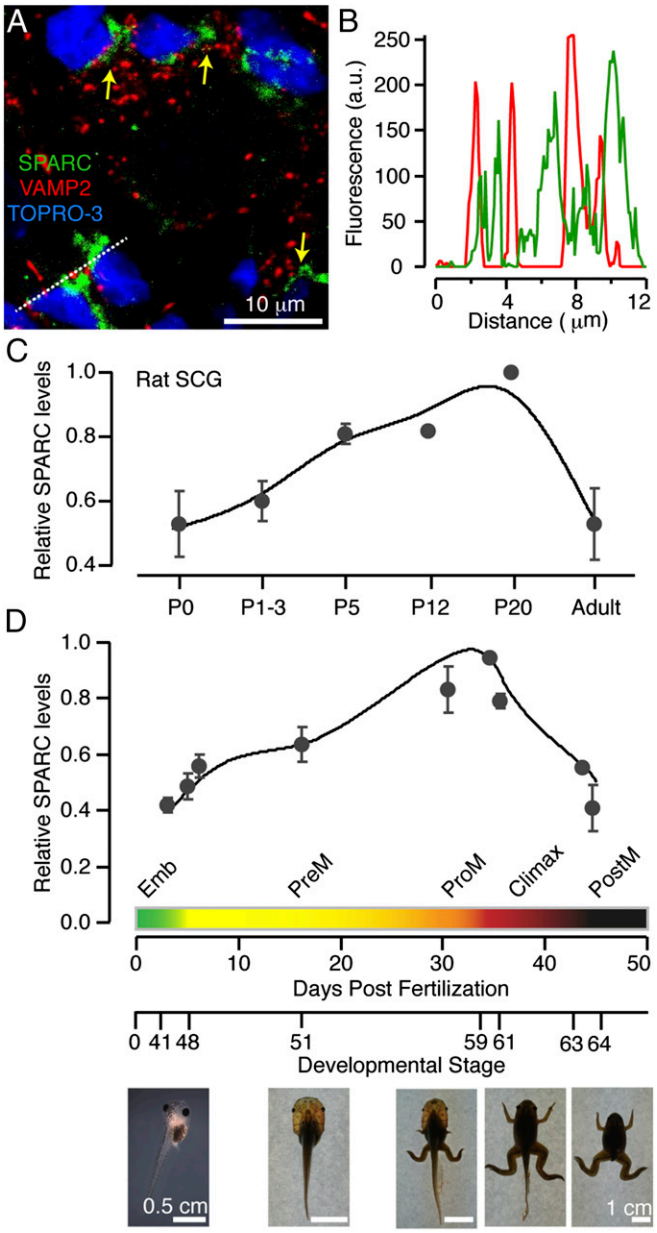

Fig. 1. Variations in SPARC production during refinement of cholinergic innervation in two different vertebrate structures. (*A*) Section of a rat superior cervical ganglion at postnatal day 20 showing SPARC accumulates around putative presynaptic terminals labeled with VAMP2 (arrows). (*B*) Plot profile of VAMP2 and SPARC fluorescence intensities measured from the dotted line shown in *A*). (*C*) Relative SPARC expression in the rat superior cervical ganglion at the indicated postnatal days. (*D*) Relative changes in SPARC levels in the tails of *X. tropicalis* during normal development. The relationship of Nieuwkoop–Faber stages to days postfertilization is indicated. Images show the characteristic morphology of tadpoles at the stages of embryogenesis (Emb), premetamorphosis (PreM), prometamorphosis (ProM), metamorphosis climax, and postmetamorphosis (PostM). Data in *C* and *D* are mean ± SEM.

for the innervation of other cholinergic vertebrate structures as well. The tails of *Xenopus* larvae offer an ideal window in which to evaluate this possibility, because multiple neuromuscular junctions are formed and eliminated following a stereotyped program (20). In agreement with previous observations in *X. laevis* (21), SPARC levels were minimal at the end of *Xenopus tropicalis* embryogenesis, when tadpole swimming is exclusively driven by tail movements [Nieuwkoop–Faber (NF) stage 40–52] (Fig. 1*D* and Fig. S1). As development progressed, SPARC levels increased constantly and reached a peak just before the climax of metamorphosis (NF stage 59–60). At this stage, tadpoles switch to leg swimming, tail resorption program starts (22), the primary motor neuron pool controlling tail movements is eliminated, and the secondary motor neuron pool begins to drive limb locomotion (23). Along with our findings in rat superior cervical ganglion, our observations support the idea that maximal SPARC production occurs concomitantly with synapse elimination in cholinergic vertebrate structures.

SPARC Inhibits Formation of Cholinergic Synapses. We investigated the direct involvement of SPARC on synapse elimination using SCMs obtained from the rat superior cervical ganglion (15), which allowed us to investigate fast cholinergic neurotransmission in the absence of glia. Application of SPARC at 5–25 nM throughout the entire period of synaptogenesis (Fig. 2*A*) decreased synaptic responses in a concentration-dependent manner. Although the characteristic onset of neurotransmission at ∼12 d in vitro was unaffected, quantification of functional synapses from recorded microcultures supports the idea that SPARC interfered with their development. For example, exposure to 25 nM SPARC caused a threefold decrease in the density of mature presynaptic terminals (Fig. 2*B*), from 0.1 ± 0.04 bassoon puncta·μm^2 (n = 14) to 0.03 ± 0.005 bassoon puncta·μm^2 (n = 6).

Full-length SPARC contains three distinct conserved domains (Fig. 2*C*): NH2-terminal acidic domain, follistatin-like (FS) domain, and the C-terminal (EC) domain. To identify the protein region responsible for synaptic effects, taking into account that FS and EC domains mediate most SPARC actions, we used peptide 2.1 (p2.1) and peptide 4.2 (p4.2), which derive from FS and EC domains, respectively. Both peptidic sequences are active on nonneuronal cells, showing comparable properties to the full-length protein, such as disruption of focal adhesions (24). To examine whether selected peptides were also acting on synapses, we assessed their additive effect on recombinant SPARC. p2.1 and p4.2 were applied in combination with 5 nM SPARC, a concentration that does not affect the amplitude of synaptic responses, but arrests terminals at an immature stage (14). The addition of 50 nM p2.1 and 5 nM SPARC did not change the amplitude of excitatory postsynaptic currents (EPSCs; Fig. 2*D*); however, synaptic responses were reduced when SPARC was combined in a 1:10 ratio with p4.2. The effect was reminiscent of that seen on 25 nM SPARC application (Fig. 2 *B* and *D*).

Actually, p4.2 retained SPARC actions, as shown by the reduction of EPSC amplitude at $[p4.2]_{50}$ of ∼14 nM, almost identical to the $[SPARC]_{50}$ of ∼13 nM (Fig. 2*E*). Application of p4.2 alone also caused a concentration-dependent decrease in the density of mature presynaptic terminals (Fig. 2*F*). In contrast, p2.1 was completely ineffective. Taken together, our results show that p4.2 is an active, inhibitory peptide of synaptogenesis, displaying an analogous effect to full-length SPARC.

p4.2 Triggers Cell-Autonomous Elimination of Cholinergic Synapses. To assay the activity of SPARC on fully functional synapses, we transiently incubated SCMs once in vitro development was completed (Fig. 3*A*) with SPARC-derived p2.1 (lacking synaptogenic effects) or p4.2 (inhibitor of synaptogenesis). Application of 50 nM p4.2 reduced the amplitude of synaptic currents by fourfold (Fig. 3*B*). To confirm that the decrease in synaptic currents could be attributed to a lower number of operative synapses, we stained recorded neurons for the active zone marker bassoon (Fig. 3*C*). On average, the number of functional presynaptic terminals·μm^{-2} was reduced from 0.12 ± 0.04 (n = 14) to 0.04 ± 0.01 (n = 21). Neither neurotransmission nor the number of synaptic contacts was affected when p2.1 was applied. The effects of 50 nM p4.2 were significant only when the incubation time was 24–48 h; for shorter periods (i.e., 4–6 h), it was necessary to increase [p4.2] up

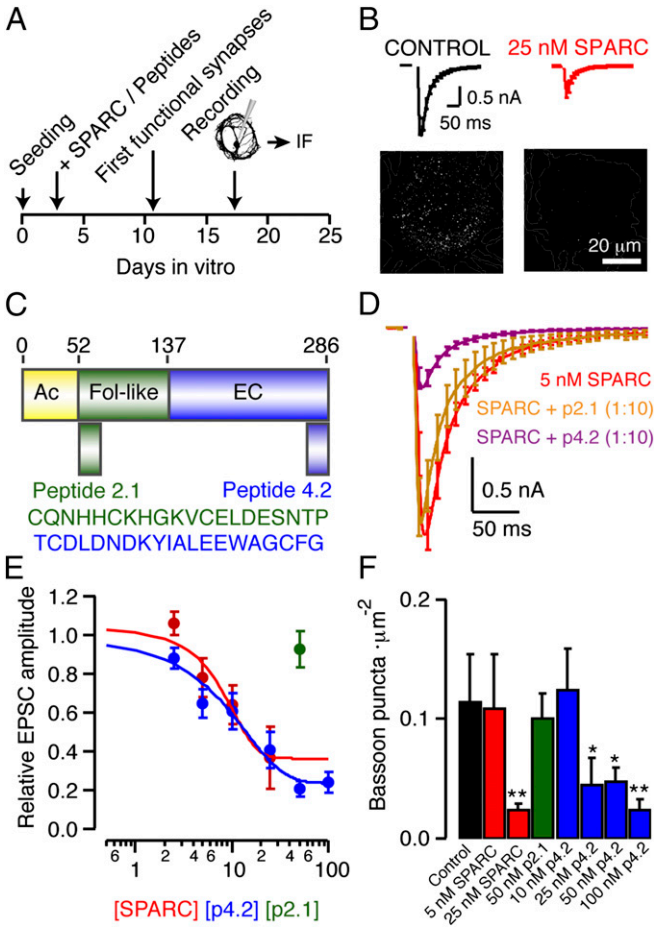

Fig. 2. Identification and mapping of the functional SPARC region inhibiting synaptic development. (*A*) Schematic diagram of the experimental procedure used to investigate the inhibitory role of SPARC throughout the whole period of synapse formation and maturation. The time course of in vitro synaptic development is indicated. (*B*) Effect of SPARC on evoked autaptic currents and the density of presynaptic terminals, visualized as bassoon puncta. (*C*) Amino acid sequence and location of p2.1 and p4.2 in the full-length protein. (*D*) Average EPSC of neurons developed in the presence of 5 nM SPARC ($n = 24$), 5 nM SPARC + 50 nM p2.1 ($n = 8$), and 5 nM SPARC + 50 nM p4.2 ($n = 29$). (*E*) Relative decay in EPSC amplitude as a function of SPARC or p4.2. Sigmoidal fits of averaged data (from 6–24 independent observations) revealed $[SPARC]_{50}$ and $[p4.2]_{50}$ of 13 nM and 14 nM, respectively. The absence of inhibition by 50 nM p2.1 ($n = 6$) is also indicated. (*F*) Summary of SPARC-derived peptides on the density of bassoon puncta (control, $n = 14$; 5 nM SPARC, $n = 10$; 25 nM SPARC, $n = 6$; 50 nM p2.1, $n = 5$; 10 nM p4.2, $n = 12$; 25 nM p4.2, $n = 7$; 50 nM p4.2, $n = 17$; 100 nM p4.2, $n = 6$). All averages are presented as mean ± SEM. $*P < 0.01$; $**P < 0.001$.

to 200 nM to obtain reductions in synaptic currents and presynaptic terminal density. The decrease in EPSC amplitude was concentration-dependent (Fig. 3*D*) and occurred with a half-time of ∼4 h (Fig. S2). Considering the minimal synapse formation in mature cultures (14), this time course of inhibition supported the idea that existing contacts were being disassembled. The effect of p4.2 was blocked when applied in combination with jasplakinolide, a drug that stabilizes actin filaments but remained unaltered in the presence of tetrodotoxin (TTX; Fig. 3*D*). Therefore, the p4.2-triggered loss of synaptic contacts was activity-independent and presumably involved disruption of the actin cytoskeleton.

To visualize how the morphology of mature synapses was affected by acute application (6 h) of SPARC peptides, we inspected some of the recorded microcultures by electron microscopy. Control presynaptic terminals showed prominent active zones and numerous cytoplasmic vesicles (Fig. 3*E*). Exposure to 200 nM p4.2 increased the number of endocytic shapes and invaginations in the vicinity of active zones more than threefold (Fig. 3*F* and Fig. S3). Hallmarks of endocytosis were increased at the postsynaptic level as well (Fig. 3*G*). In some synapses, characteristic cup-shaped membrane invaginations, which were absent from controls, became evident when presynaptic and postsynaptic omega-shapes occurred simultaneously (Fig. 3 *H* and *I* and Fig. S3). Tightly coupled presynaptic and postsynaptic invaginations, together with the increase in endocytic shapes, suggested that synaptic contacts were detaching.

Further evidence favoring the onset of a program of synapse elimination was the formation of large endosomal structures. Only 6% ($n = 49$) of control presynaptic terminals showed large endocytic compartments at rest. However, on acute exposure to 200 nM p4.2, multivesicular bodies were observed in 53% of terminals inspected ($n = 40$; Fig. 3*J*). Large endosomes were formed in a cell-autonomous manner and occurred in different shapes and sizes, all containing diverse axonal material (Fig. S3). Concomitant with the formation of multivesicular bodies, lysosomal activity was enhanced. Lysosomes increased in size by 30% (Fig. 4*A*) and were observed in 28% ($n = 40$) of presynaptic terminals. Putative secondary lysosomes were found in terminals showing a normal morphology and terminals resembling retracting axon tips (Fig. 4 *B–D* and Fig. S3). Incubation of SCMs with LysoTracker red showed that the density of these acidic compartments was essentially unaffected by exposure to any of the SPARC peptides; however, differences in size were obvious (Fig. S4). Acute exposure to p4.2 increased the perimeter of lysosomes by twofold, reinforcing electron microscopy data and suggesting that p4.2 induces the transition from primary to secondary lysosomes. Together, the optical and electron microscopy data describe an in vitro phenotype resembling some aspects of the developmental elimination of synaptic inputs in the mouse neuromuscular junction, characterized by increased lysosomal activity (8).

p4.2 Triggers Elimination of Neuromuscular Junctions in Vivo. We used *X. tropicalis* tadpoles to investigate the relevance of a SPARC-mediated program of synapse elimination in vivo. SPARC secretion is developmentally regulated in the tadpole tail, such that the lowest protein levels are found during embryogenesis and premetamorphosis (Fig. 1*D*). In the developmental period at NF stage 48–54 (25), limbs are not present and swimming is controlled exclusively by tail beats, which occur at ∼3 Hz (Fig. 5*A*). The characteristic motor behavior of tadpoles alternating continuous swimming with idle times (Movie S1) was unaffected after microinjection at the somite level of 300 pmol of p2.1, but was impaired when the same amount of p4.2 was applied (Fig. 5*B* and Movie S2). Effect was evident at 5 h after injection, when peptide was distributed homogenously throughout the tail (Fig. S5). During this acute phase, tails were completely straight (Fig. 5*A*), inducing a characteristic resting side position in some animals. Tadpoles injected with p4.2 had swimming periods of just a few seconds. They appeared fatigued and rapidly returned to an inactive state, likely reflecting the inability to recruit all tail muscles (Movie S2). The average swimming speed of 2.6 ± 0.22 mm·s^{-1} seen in p2.1-injected tadpoles ($n = 80$) was decreased to 1.6 ± 0.19 mm·s^{-1} in those injected with p4.2 ($n = 80$; $P = 0.0016$) (Fig. 5*C*).

Motor deficits did not alter normal development, and tadpoles progressed to the stage of prometamorphosis. Growth was unaffected because virtual paralysis was restricted to a time window of 48 h after peptide injection (Fig. 5*B*). The lack of motor movements controlled at the spinal cord level contrasted with apparently normal buccal pumping and heartbeat, 71 ± 5 pumps·min^{-1} ($n = 13$) and 112 ± 6 beats·min^{-1} ($n = 12$), similar to previously reported values (26). The normal autonomic functions suggest that rostral portions of central nervous system connectivity were not targeted by peptide injections. The correct processing of mechanosensitive

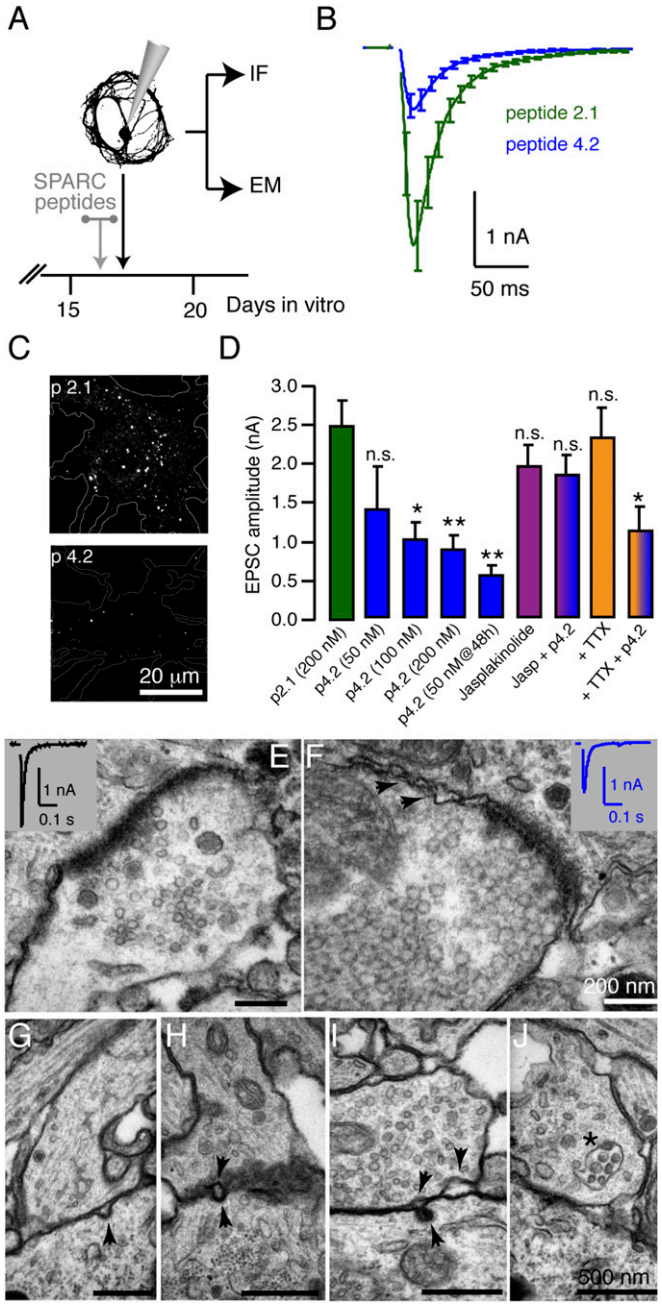

Fig. 3. SPARC p4.2 triggers the disassembly of mature cholinergic synapses. (*A*) Experimental protocol used to investigate the role of SPARC-derived peptides on the activity of stable autapses. (*B*) Average EPSCs of mature neurons acutely exposed to p2.1 ($n = 8$) or p4.2 ($n = 33$). (*C*) p4.2 decreased the number of functional presynaptic terminals measured as bassoon puncta. (*D*) The amplitude of postsynaptic responses decreased as a function of p4.2. Exposure to p2.1 did not modify EPSC amplitude. All peptides were incubated for 4–6 h before recording. Note that the effect of p4.2 was inhibited by jasplakinolide, but remained unchanged when firing of action potentials was blocked by TTX (200 nM p2.1, $n = 13$; 50 nM p4.2, $n = 18$; 100 nM p4.2, $n = 6$; 200 nM p4.2, $n = 16$, 1 μM jasplakinolide, $n = 11$; 1 μM jasplakinolide + 200 nM p4.2, $n = 12$; 20 nM TTX, $n = 6$; 20 nM TTX + 200 nM p4.2, $n = 8$). (*E*) Image of a control presynaptic terminal from a recorded autaptic neuron (*Inset*). (*F*) Image from a presynaptic terminal acutely treated with p4.2. Arrows indicate membrane invaginations near an active zone. (*G–J*) Images from four different synapses treated with p4.2. Note the presence of presynaptic and postsynaptic endocytic profiles (arrows). (*J*) A presynaptic terminal containing a multivesicular body (asterisk). All averages are presented as mean ± SEM. $*P < 0.01$; $**P < 0.001$.

stimuli activating lateral line and trigeminal receptors (27) reinforces this view, because occasional collisions among tadpoles or external mechanical stimuli always activated a response driven by tail swim. Thus, the normal hindbrain-mediated responses indicate that p4.2 injections at the tail level were restricted to spinal cord connectivity, without affecting upper neuronal structures.

Peptides were completely cleared from tadpole tails by 24–48 h after injection (Fig. S5). Spontaneous tail oscillations became evident at 3 d after p4.2 injection. Characteristic tail flickering reappeared for short periods, and inactivity time was decreased (Movie S3); however, swimming was not spontaneous and was evoked only by mechanical stimuli. At 6 d after injection, tadpoles exhibited the characteristic motility associated with their developmental stage (Fig. 5*D* and Movie S4).

We investigated the nature of motor deficits observed after p4.2 injection by staining tadpole tails for acetylated tubulin and synaptophysin to label axonal tracts and presynaptic terminals, respectively. Motor axons emanating from the spinal cord branched along the tail, forming numerous neuromuscular junctions (Fig. 5*E*), likely polyinnervating muscle fibers (28). The characteristic distribution of neuromuscular synapses was unaffected by injection of p2.1 peptide; however, connectivity was completely altered in tadpoles showing severely impaired swimming behavior after p4.2 injection. Most of the tail neuromuscular junctions were absent, and the average thickness of axon branches (measured as the FWHM from line profiles) was increased from 1.8 ± 0.05 μm ($n = 580$) to 3.2 ± 0.05 μm ($n = 212$; $P < 0.001$), suggesting a pruning process (Fig. 5*E* and Fig. S6). Elimination of axons was noted on confocal and light-sheet microscopy, and putative retraction bulbs were observed (Movies S5 and S6). Improvement in swimming ability occurred when neuromuscular junctions reformed by 6 d after p4.2 injection (Fig. 5*E*) and thin axon branches (average FWHM, 1.8 ± 0.2 μm; $n = 51$) became evident again (Fig. S6 and Movie S7).

Discussion

Matricellular proteins, such as SPARC, are maximally produced during a restricted time window of normal development (29). We have shown that in vertebrate cholinergic structures, SPARC levels peak when connectivity is refined (Fig. 1). By acting through a peptidic sequence located in its EC domain (Fig. 2), SPARC triggers disassembly of presynaptic and postsynaptic terminals (Fig. 3), setting the onset of a neuronal, cell-autonomous program of synapse elimination. As synaptic contacts retract, multivesicular

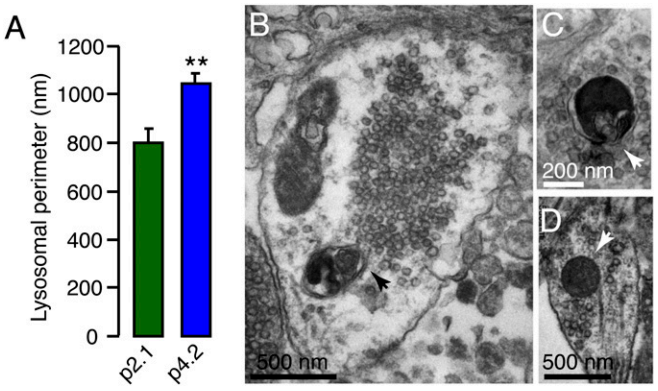

Fig. 4. SPARC p4.2 activates the formation of secondary lysosomes in mature presynaptic terminals. (*A*) Lysosomes of neurons treated for 6 h with 200 nM p4.2 ($n = 49$) are larger than those found after acute exposure to 200 nM p2.1 ($n = 40$). (*B*) A secondary lysosome located in a presynaptic terminal treated with p4.2 (arrow). (*C*) A secondary lysosome formed by fusion to a multivesicular body. (*D*) A lysosome found in a retracting axon terminal. Averages are presented as mean ± SEM. $**P < 0.001$.

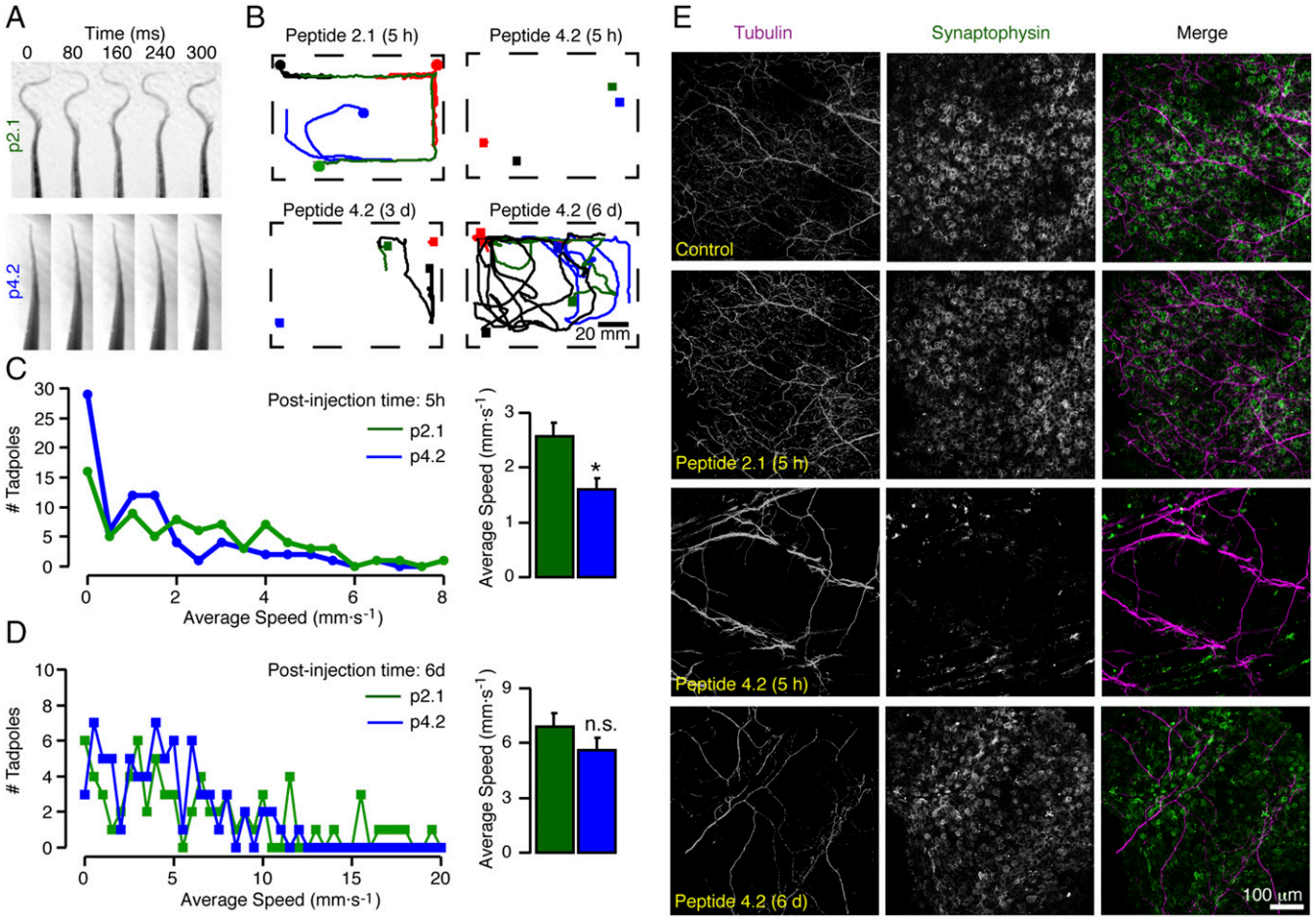

Fig. 5. SPARC p4.2 induces retraction of motor neuron axons and impairs tadpole swimming. (*A*) Images from tadpole tails showing how the characteristic ~3-Hz tail beat is blocked by local injection with p4.2 but is unaffected by p2.1. (*B*) Swimming activity integrated over 30 s. Motor behavior is transiently affected by p4.2, shown by tracking movements of four different tadpoles (squares) at three consecutive time points: 5 h, 3 d, and 6 d. Swimming is unaffected by p2.1 (Movies S1–S4). (*C*) Distribution and mean average speed (mean ± SEM; $P < 0.01$) of tadpoles at 5 h after injection with p2.1 ($n = 80$) or p4.2 ($n = 80$). (*D*) Same as *C* but at 6 d after injection with p2.1 ($n = 76$) or p4.2 ($n = 78$; $P = 0.16$). (*E*) Staining of *X. tropicalis* tadpole tails for acetylated tubulin and synaptophysin to indicate the location of axons and presynaptic terminals, respectively. Note how neuromuscular junctions virtually disappear at 5 h after p4.2 injection but become evident within 6 d.

bodies are generated and digested by lysosomes (Fig. 4), driving the loss of functional innervation (Fig. 5).

Our results support a fundamental role for the secretory activity of glial cells during refinement of neuronal circuit connectivity. Along with favoring the establishment of synaptic contacts by releasing synaptogenic factors, such as thrombospondin, glypicans, and hevin (9–11), glia, through SPARC secretion, also can inhibit formation and consolidation of synaptic contacts. Based on previously reported and current in vitro evidence, the effects are concentration-dependent and range from arresting maturation of presynaptic terminals (14) to eliminating these terminals. However, the effective SPARC concentration in a biologically relevant context, and thus its specific inhibitory action, would be determined by at least three factors: (*i*) the quantity and location of secretory events in glial processes relative to synapses (14); (*ii*) the presence of competitive antagonists, such as hevin (10); and (*iii*) cleavage by matrix metalloproteases. Exposure of full-length SPARC to collagenase-3, gelatinase A, gelatinase B, and matrilysin releases a 91-aa peptide containing p4.2 (30). In light of our results, such a fragment could mimic the synaptic actions of SPARC and thus increase the effective protein concentration in the extracellular space.

The onset of a program of synapse elimination triggered by SPARC also depends on the expression of a specific neuronal receptor. A possible candidate is the integrin α5β1 complex, which binds p4.2 (31) and is expressed in *Xenopus* neuromuscular active zones (32). In nonneuronal cells, interaction of SPARC with β1 integrin complexes linked to cytoskeletal proteins, such as talin and actin, mediates the loss of focal adhesions (24, 31, 33). In vitro results using jasplakinolide suggest an analogous mechanism in synapses, through which depolymerization of synaptic F-actin cytoskeleton may lead to disruption of active zones and disorganization of synaptic vesicle pools (34, 35). The resulting presynaptic endosomal structures could be digested within neurons; however, it is possible that in vivo activation of same program would ultimately involve phagocytosis by glial cells, i.e., axosome shedding (2). Alternatively, SPARC could cause the pruning of axonal branches through protein–protein interactions with the cytoskeleton. Some evidence supports protein internalization via clathrin-mediated endocytosis (36), which could allow interaction with cytoskeletal elements, such as α-tubulin (37). Whether this interaction leads to the elimination of microtubules is unknown; however, an action of SPARC requiring its internalization is also supported by the results with jasplakinolide, given that stabilization of the actin cytoskeleton disrupts receptor-mediated endocytosis (38).

Although the action of p4.2 remained unaffected when neuronal activity was silenced with TTX, we cannot rule out a relationship between SPARC's effect and neuronal firing patterns. For example, changes in synaptic activity could drive the

heterogeneous distribution of putative SPARC receptors, by altering the expression of particular integrin-β1 complexes (39) or affecting clathrin-mediated endocytosis (40). In this way, subsets of synapses would be at greater or lesser risk of being eliminated. This scenario could be relevant for neuromuscular junctions, because SPARC is distributed throughout the endomysium (41) (Fig. S7). The capacity of glial cells to sense neuronal activity during development should be taken into account as well (42). Terminal Schwann cells compete for perysinaptic space during development (43) and are capable of deciphering between weak and strong inputs by differentially increasing their free $[Ca^{2+}]$ (44). Thus, changes in glial free $[Ca^{2+}]$ could affect protein secretion from glia, either by promoting exocytosis or by altering transcriptional control.

Taken together, our results prompt us to consider SPARC as a trigger for cholinergic synapse elimination. Along with constitutively engulfing axonal debris (3, 43), glial cells release SPARC in a timely manner to determine the fate of synaptic contacts.

Materials and Methods

All animal procedures were approved by the Department of Environment at Generalitat de Catalunya. Procedures for establishing SCMs from superior cervical ganglion neurons and correlative electrophysiology and optical or electron microscopy have been described elsewhere (14, 15). Detailed protocols for experiments involving SCMs, maintenance of the *X. tropicalis* colony, injections of SPARC- derived peptides at the somite level, analysis of tadpole swimming, quantification of SPARC levels, and whole-mount immunohistochemistry are provided in *SI Materials and Methods*.

For statistical analysis, the unpaired Student *t* test was used to evaluate differences between two experimental groups. Comparisons among three or more groups was performed using one-way ANOVA, followed by the Bonferroni post hoc test.

ACKNOWLEDGMENTS. We thank the Electron Microscopy Unit (Campus Casanova) of Centres Científics i Tecnològics of the University of Barcelona for their involvement and support, the National Xenopus Resource (Woods Hole, MA), and Daniel Colon-Ramos for his valuable comments. This work was supported by grants from El Ministerio de Economía y Competitividad (MINECO; SAF 2012-36375) cofunded by the European Regional Development Fund (ERDF), Fundació La Marató de TV3 (111530) (to A.L.), and by competitive research awards from the M. G. F. Fuortes Memorial Fellowship, the Stephen W. Kuffler Fellowship Fund, the Laura and Arthur Colwin Endowed Summer Research Fellowship Fund, the Fischbach Fellowship, and the Great Generation Fund of the Marine Biological Laboratory, where a portion of this work was conducted under the auspices of these awards. F.J.L.-M. was a recipient of a MINECO predoctoral fellowship (BES-2010-032355).

1. Watts RJ, Schuldiner O, Perrino J, Larsen C, Luo L (2004) Glia engulf degenerating axons during developmental axon pruning. *Curr Biol* 14(8):678–684.
2. Bishop DL, Misgeld T, Walsh MK, Gan WB, Lichtman JW (2004) Axon branch removal at developing synapses by axosome shedding. *Neuron* 44(4):651–661.
3. Chung WS, et al. (2013) Astrocytes mediate synapse elimination through MEGF10 and MERTK pathways. *Nature* 504(7480):394–400.
4. Smith IW, Mikesh M, Lee Yi, Thompson WJ (2013) Terminal Schwann cells participate in the competition underlying neuromuscular synapse elimination. *J Neurosci* 33(45): 17724–17736.
5. Schafer DP, et al. (2012) Microglia sculpt postnatal neural circuits in an activity and complement-dependent manner. *Neuron* 74(4):691–705.
6. Stevens B, et al. (2007) The classical complement cascade mediates CNS synapse elimination. *Cell* 131(6):1164–1178.
7. Stephan AH, Barres BA, Stevens B (2012) The complement system: An unexpected role in synaptic pruning during development and disease. *Annu Rev Neurosci* 35:369–389.
8. Song JW, et al. (2008) Lysosomal activity associated with developmental axon pruning. *J Neurosci* 28(36):8993–9001.
9. Christopherson KS, et al. (2005) Thrombospondins are astrocyte-secreted proteins that promote CNS synaptogenesis. *Cell* 120(3):421–433.
10. Kucukdereli H, et al. (2011) Control of excitatory CNS synaptogenesis by astrocyte-secreted proteins Hevin and SPARC. *Proc Natl Acad Sci USA* 108(32):E440–E449.
11. Allen NJ, et al. (2012) Astrocyte glypicans 4 and 6 promote formation of excitatory synapses via GluA1 AMPA receptors. *Nature* 486(7403):410–414.
12. Vincent AJ, Lau PW, Roskams AJ (2008) SPARC is expressed by macroglia and microglia in the developing and mature nervous system. *Dev Dyn* 237(5):1449–1462.
13. Jones EV, et al. (2011) Astrocytes control glutamate receptor levels at developing synapses through SPARC–beta-integrin interactions. *J Neurosci* 31(11):4154–4165.
14. Albrecht D, et al. (2012) SPARC prevents maturation of cholinergic presynaptic terminals. *Mol Cell Neurosci* 49(3):364–374.
15. Perez-Gonzalez AP, Albrecht D, Blasi J, Llobet A (2008) Schwann cells modulate short-term plasticity of cholinergic autaptic synapses. *J Physiol* 586(Pt 19):4675–4691.
16. Rubin E (1985) Development of the rat superior cervical ganglion: Initial stages of synapse formation. *J Neurosci* 5(3):697–704.
17. Aguayo AJ, Peyronnard JM, Terry LC, Romine JS, Bray GM (1976) Neonatal neuronal loss in rat superior cervical ganglia: Retrograde effects on developing preganglionic axons and Schwann cells. *J Neurocytol* 5(2):137–155.
18. Lichtman JW, Purves D (1980) The elimination of redundant preganglionic innervation to hamster sympathetic ganglion cells in early post-natal life. *J Physiol* 301: 213–228.
19. Martinek N, Zou R, Berg M, Sodek J, Ringuette M (2002) Evolutionary conservation and association of SPARC with the basal lamina in *Drosophila*. *Dev Genes Evol* 212(3): 124–133.
20. Combes D, Merrywest SD, Simmers J, Sillar KT (2004) Developmental segregation of spinal networks driving axial- and hindlimb-based locomotion in metamorphosing *Xenopus laevis*. *J Physiol* 559(Pt 1):17–24.
21. Damjanovski S, Malaval L, Ringuette MJ (1994) Transient expression of SPARC in the dorsal axis of early *Xenopus* embryos: Correlation with calcium-dependent adhesion and electrical coupling. *Int J Dev Biol* 38(3):439–446.
22. Brown DD, Cai L (2007) Amphibian metamorphosis. *Dev Biol* 306(1):20–33.
23. Forehand CJ, Farel PB (1982) Spinal cord development in anuran larvae, I: Primary and secondary neurons. *J Comp Neurol* 209(4):386–394.
24. Murphy-Ullrich JE, Lane TF, Pallero MA, Sage EH (1995) SPARC mediates focal adhesion disassembly in endothelial cells through a follistatin-like region and the Ca(2+)-binding EF-hand. *J Cell Biochem* 57(2):341–350.
25. Nieuwkoop PD, Faber J, eds (1956) *Normal Table of* Xenopus laevis *(Daudin): A Systematical and Chronological Survey of the Development From the Fertilized Egg Till the End of Metamorphosis* (North-Holland, Amsterdam), p 243.
26. Eckelt K, Masanas H, Llobet A, Gorostiza P (2014) Automated high-throughput measurement of body movements and cardiac activity of *Xenopus tropicalis* tadpoles. *J Biol Methods* 1(2):e9.
27. Buhl E, Roberts A, Soffe SR (2012) The role of a trigeminal sensory nucleus in the initiation of locomotion. *J Physiol* 590(Pt 10):2453–2469.
28. Lannoo M (1999) Integration: Nervous and sensory systems. *The Biology of Anuran Larvae,* eds McDiarmid R, Altig R (Univ of Chicago Press, Chicago), pp 149–169.
29. Murphy-Ullrich JE, Sage EH (2014) Revisiting the matricellular concept. *Matrix Biol* 37:1–14.
30. Sasaki T, et al. (1997) Limited cleavage of extracellular matrix protein BM-40 by matrix metalloproteinases increases its affinity for collagens. *J Biol Chem* 272(14):9237–9243.
31. Nie J, et al. (2008) IFATS collection: Combinatorial peptides identify alpha5beta1 integrin as a receptor for the matricellular protein SPARC on adipose stromal cells. *Stem Cells* 26(10):2735–2745.
32. Cohen MW, Hoffstrom BG, DeSimone DW (2000) Active zones on motor nerve terminals contain alpha 3beta 1 integrin. *J Neurosci* 20(13):4912–4921.
33. Weaver MS, Workman G, Sage EH (2008) The copper binding domain of SPARC mediates cell survival in vitro via interaction with integrin beta1 and activation of integrin-linked kinase. *J Biol Chem* 283(33):22826–22837.
34. Nelson JC, Stavoe AK, Colón-Ramos DA (2013) The actin cytoskeleton in presynaptic assembly. *Cell Adhes Migr* 7(4):379–387.
35. Goda Y, Davis GW (2003) Mechanisms of synapse assembly and disassembly. *Neuron* 40(2):243–264.
36. Nakamura K, Yamanouchi K, Nishihara M (2014) Secreted protein acidic and rich in cysteine internalization and its age-related alterations in skeletal muscle progenitor cells. *Aging Cell* 13(1):175–184.
37. Huynh MH, Sodek K, Lee H, Ringuette M (2004) Interaction between SPARC and tubulin in *Xenopus*. *Cell Tissue Res* 317(3):313–317.
38. Yarar D, Waterman-Storer CM, Schmid SL (2005) A dynamic actin cytoskeleton functions at multiple stages of clathrin-mediated endocytosis. *Mol Biol Cell* 16(2): 964–975.
39. Lin CY, Lynch G, Gall CM (2005) AMPA receptor stimulation increases alpha5beta1 integrin surface expression, adhesive function and signaling. *J Neurochem* 94(2): 531–546.
40. López-Murcia FJ, Royle SJ, Llobet A (2014) Presynaptic clathrin levels are a limiting factor for synaptic transmission. *J Neurosci* 34(25):8618–8629.
41. Hoffman EP, Brown RH, Jr, Kunkel LM (1987) Dystrophin: The protein product of the Duchenne muscular dystrophy locus. *Cell* 51(6):919–928.
42. Darabid H, Perez-Gonzalez AP, Robitaille R (2014) Neuromuscular synaptogenesis: Coordinating partners with multiple functions. *Nat Rev Neurosci* 15(11):703–718.
43. Brill MS, Lichtman JW, Thompson W, Zuo Y, Misgeld T (2011) Spatial constraints dictate glial territories at murine neuromuscular junctions. *J Cell Biol* 195(2):293–305.
44. Darabid H, Arbour D, Robitaille R (2013) Glial cells decipher synaptic competition at the mammalian neuromuscular junction. *J Neurosci* 33(4):1297–1313.